Ring of the University of Wisconsin Synchrotron Radiation Center which is supported by National Science Foundation Grant No. DMR-74-15089.

[1]N. D. Lang and A. R. Williams, Phys. Rev. Lett. 37, 212 (1976).

[2]For a more detailed discussion of the CFS technique see G. J. Lapeyre, A. D. Baer, J. Hermanson, J. Anderson, J. A. Knapp, and P. L. Gobby, Solid State Commun. 15, 1601 (1974). See also Z. Hurych, J. C. Shaffer, D. L. Davis, T. A. Knecht, G. J. Lapeyre, P. L. Gobby, J. A. Knapp, and C. G. Olson, Phys. Rev. Lett. 33, 830 (1974).

[3]W. Gudat and C. Kunz, Phys. Rev. Lett. 29, 169 (1972).

[4]R. L. Benbow and Z. Hurych, Phys. Rev. B 14, 4295 (1976).

[5]It has been indicated that the splitting of the VB of Bi into peaks labeled $6p_{1/2}$ and $6p_{3/2}$ is due *primarily* to the SO interaction. L. Ley, R. A. Pollak, S. Kowalczyk, F. R. McFeely, and D. A. Shirley, Phys. Lett. 41A, 429 (1972), and Phys. Rev. B 8, 641 (1973), and references therein.

[6]Similar SO structure in the CBODOS has been reported previously in Bi_2Te_3. Hurych *et al.*, Ref. 2.

[7]The relative strengths of the empty $p_{1/2}$- and $p_{3/2}$-like peaks are difficult to estimate since the two peaks are overlapping, but some qualitative estimates can still be made. Two facts indicate a sharp maximum of the empty $p_{1/2}$-like DOS: (i) The transition $d_{5/2} \rightarrow p_{1/2}$ of a very small matrix element (zero for atomiclike case) is clearly discernible as the peak X, and (ii) the transition of $d_{3/2} \rightarrow p_{1/2}$ (peak Z) dominates the spectrum despite having smaller atomic matrix element (see Table I) than the $d_{5/2} \rightarrow p_{3/2}$ transition (peak Y).

[8]Observation of the above features of the CBODOS in all Bi chalcogenides and lack of these features in Sb_2Te_3 (which has the same crystal structure as Bi_2Te_3) suggest that the SO splitting rather than the crystal-field effects is the dominant factor in determining the above features of CBODOS in Figs. 1 and 3. Likewise, the fact that the sharpest structures in Fig. 3 occur for (presumably) polycrystalline Be_2O_3, grown on polycrystalline Bi films, rather than for single crystals of Bi_2Te_3 or Bi_2Se_3, supports our interpretation of the CBODOS (Fig. 3) in terms of partial ionicity.

[9]J. R. Drabble and C. H. Goodman, J. Phys. Chem. Solids 5, 142 (1958).

[10]G. Martinez, M. Schluter, M. L. Cohen, R. Pinchaux, P. Thiry, D. Dagneaux, and Y. Petroff, Solid State Commun. 17, 5 (1975), and references therein.

Selection Rules in Raman Scattering from Surface Polaritons

J. B. Valdez and S. Ushioda
Department of Physics, University of California, Irvine, California 92717
(Received 14 February 1977)

Raman-scattering selection rules for surface polaritons have been studied by experiments using a thin (≈ 20 μm) single-crystal slab of GaP of known orientation. The dispersion of the observed mode has been determined by varying the scattering angle, and comparison is made with the theoretically predicted dispersion of surface polaritons at the surface of a semi-infinite GaP crystal. The observed selection rules are consistent with the results of an analysis using the bulk Raman tensors.

Recently, surface polaritons (SP) have been observed by Raman scattering from polycrystalline films of GaAs.[1] In these experiments, the authors observed scattering from the upper and lower SP modes characteristic of a two-interface, or slab, configuration where the thickness of the slab is comparable to the penetration depth of the surface mode.[2] Thus far, however, no successful observations have been made of Raman scattering from SP with a single crystal of known orientation. Consequently, the polarization selection rules for SP have not previously been determined. We report in this Letter the first determination of Raman-scattering selection rules for surface polaritons.

We have performed near-forward Raman scattering measurements on a thin (≈ 20 μm) slab of single-crystal GaP with (111) faces with known orientation in the plane. A peak in the Raman spectrum has been observed, whose frequency lies between the bulk TO and LO phonon frequencies for GaP (367.3 and 403.0 cm^{-1}, respectively). In order to identify this mode as being the SP, we determined its dispersion by varying the scattering angle, and compared it with the theoretical dispersion of SP at a single GaP-air interface.[3] We then determined a set of selection rules for the scattering by varying the polarization of the incident light and the direction and polarization of the observed scattered light.

The GaP samples which we used in this study were prepared by cutting oriented rectangular parallepipeds, $\approx 2.5 \times 2.5 \times 1$ mm^3, from a single-crystal boule supplied by H. W. Verleur. These

slabs were then ground and polished, using standard metallurgical techniques, to a final thickness of ≈ 15–25 μm. The final grit size used in the polishing was 0.05 μm. The sample on which we made the measurements reported here had a thickness of 20 μm. The exact orientation of the samples was determined by means of forward Laue x-ray photographs, which identified the [111], [$\bar{1}$10], and [$\bar{1}\bar{1}$2] directions in the crystal. (In this paper, we will refer to these directions as the $\hat{x}$, $\hat{y}$, and $\hat{z}$ axes, respectively). The Laue photographs also confirmed the single-crystalline nature of the samples.

Raman scattering measurements were made at room temperature, with the 514.5-nm line of an argon laser (≈ 400 mW) as the exciting source. The scattered light was collected by a variable-focal-length, $f/1$ lens system of our design,[4] and was analyzed by a computer-controlled double-grating spectrometer system, which has been described previously.[5] The data were recorded digitally, with typical integration times of 1 to 4 min, depending on the polarization configuration being studied. In order to define the scattering angle, various masks were placed between the crystal and the collection optics. The crystal was oriented with $\hat{x}$ parallel to the spectrometer axis, and the $\hat{y}$ and $\hat{z}$ directions were known.

In Fig. 1(a), we present a spectrum for which the scattering geometry and polarization configuration are favorable to Raman scattering from the SP, and in which the small peak due to the SP is easily visible, lying largely outside the wing of the larger peak due to the bulk LO phonon. In the general case, however, the frequency of the SP is more difficult to determine, as its intensity relative to the LO phonon peak is smaller, and furthermore, it will, for larger values of θ, lie within the LO phonon peak. For this reason, we have analyzed the data numerically in order to determine an optimum set of parameters describing both the SP and LO phonon peaks. We assumed the functional form of the data in this region to be

$$F(\omega) = a + b\omega + D_{\mathrm{LO}}(\omega) + D_{\mathrm{SP}}(\omega). \quad (1)$$

In this expression, $a + b\omega$ is the assumed form of the background, and

$$D_{\mathrm{LO,SP}}(\omega) = A_{\mathrm{LO,SP}}[(\omega_{\mathrm{LO,SP}}^2 - \omega^2)^2 + \Gamma_{\mathrm{LO,SP}}\omega^2]^{-1} \quad (2)$$

is the damped harmonic oscillator function. $\omega_{\mathrm{LO,SP}}$ is the frequency, $\Gamma_{\mathrm{LO,SP}}$ the width, and $A_{\mathrm{LO,SP}}$ the intensity of the LO phonon or the SP, respectively. The instrumental width, Γ_{inst} was ≈ 0.25 cm^{-1}, much less than the observed values of Γ_{LO} or Γ_{SP} (≈ 2–3 cm^{-1}), so that it could be neglected in this analysis. The optimum values of the parameters were determined by repeated minimization of χ^2, using the grid least-squares method.[6] In Fig. 2, we show several sets of data, obtained with the scattering angle, θ, ranging from 1.6° to 3.6° (all values quoted for θ are those measured outside the crystal). In these spectra, the polarization of the scattered light was unanalyzed, and one can see clearly the necessity of the numerical analysis which was used. The frequency of the smaller peak, as determined numerically, is indicated in each case by an arrow. The dispersion of this peak is given as a function of θ in Fig. 3. In this figure, the solid curve is the theoretical dispersion curve of a SP at the interface of a semi-infinite GaP crystal and air, given by[3]

$$K_{\parallel}^2 = (\omega^2/c^2)\{\epsilon(\omega)/[\epsilon(\omega)+1]\}^{-1}. \quad (3)$$

Here, $\vec{k}_{\parallel}$ is the wave vector of the SP parallel to the surface, ω its frequency, and c the velocity of light in vacuum. $\epsilon(\omega)$ is the frequency-dependent dielectric function of GaP.[3] In calculating $\omega(\theta)$, we have used a value of 9.091 for the high-frequency dielectric constant, ϵ_∞, which appears in $\epsilon(\omega)$.[7] Note that $k_{\parallel}$ is determined from θ by

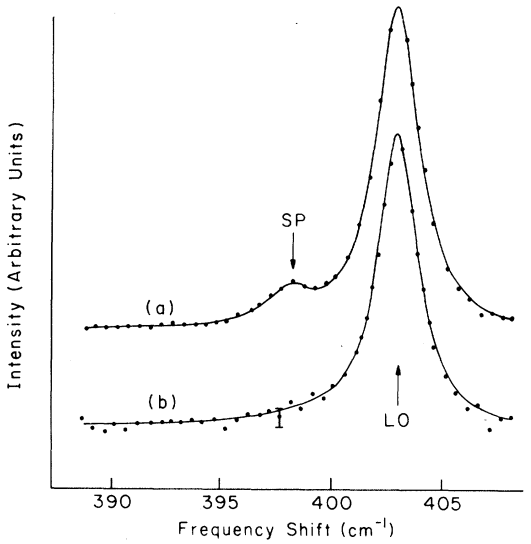

FIG. 1. Typical near-forward Raman spectra with different scattering direction and polarization configurations: (a) $\vec{k}_{\parallel} \| \hat{z}$, $\vec{E}_0 \| \hat{y}$, $\vec{E}_S \| \hat{y}$, and (b) $\vec{k}_{\parallel} \| \hat{z}$, $\vec{E}_0 \| \hat{y}$, $\vec{E}_S \| \hat{z}$. The solid curves are calculated by fitting the data (shown as dots) numerically. (SP is the surface polariton peak; LO is the LO phonon peak.)

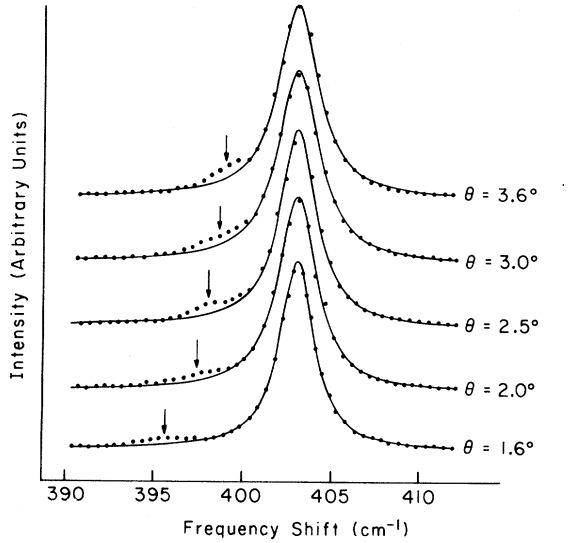

FIG. 2. Raman spectra taken with different scattering angles, θ. The dots are the experimental spectra, and the solid curves are the calculated LO-phonon contributions to the spectra. The arrow indicates the peak position of the calculated surface-polariton contribution to the data.

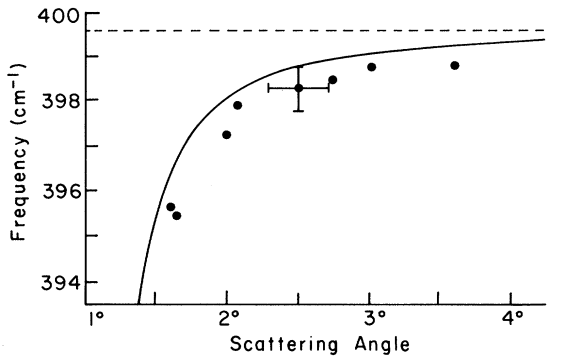

FIG. 3. Experimental dispersion of the surface polaritons SP of a 20-μm GaP slab (dots), and calculated dispersion of the semi-infinite-crystal–air interface (for $\epsilon_\infty = 9.00$). The error bars represent the combined experimental and numerical fitting uncertainties. The dashed line is the theoretical asymptotic SP frequency. Note the expanded frequency scale.

the relation

$$k_{\parallel} = 2\pi(\sin\theta)/\lambda_0, \tag{4}$$

where λ_0 is the incident light wavelength in vacuum.

In order to determine the polarization selection rules, we measured the scattering intensity for the SP at $\theta \simeq 2.5°$, for different combinations of scattering direction and incident and scattered polarizations. The intensities which we quote were determined from the least-squares parameters A_{SP}, as described earlier. We show in Fig. 1 two representative spectra obtained for different scattering configurations: (a) for $\vec{k}_{\parallel} \parallel \hat{z}$, $\vec{E}_0 \parallel \hat{y}$, $\vec{E}_S \parallel \hat{y}$, in which the SP scattering is clearly allowed, and (b) for $\vec{k}_{\parallel} \parallel \hat{z}$, $\vec{E}_0 \parallel \hat{y}$, $\vec{E}_S \parallel \hat{z}$, in which the SP scattering is evidently not allowed. Numerical analysis of these two spectra reveals that if a SP peak is present in (b), it must have a scattering intensity of $< \frac{1}{25}$ that of (a). Within experimental accuracy, we found the scattering intensity to be equal whenever $\vec{E}_0 \perp \vec{E}_S$, for a given $\vec{k}_{\parallel}$ direction, whether $\vec{E}_0 \parallel \hat{y}$ or $\hat{z}$. Likewise, for $\vec{E}_0 \parallel \vec{E}_S$ at a given $\vec{k}_{\parallel}$ direction, we found equal intensities with $\vec{E}_0 \parallel \hat{y}$ or $\hat{z}$. Our results are given in Table I, in which the numerical values represent the (relative) scattering intensities for different polarization configurations. Because $\vec{k}_0$ and $\vec{k}_S$ were both parallel to $\hat{x}$, only the configurations with $\vec{E}_0$ and $\vec{E}_S$ parallel to $\hat{y}$ and $\hat{z}$ are given.

Having determined the selection rules by experiment, we next examine the predictions of the theory. We first recall[3] that SP are elliptically polarized in the sagittal plane; i.e., there are two displacement components, 90° out of phase. These components are $\vec{u}_{\perp}$ (parallel to the surface normal) and $\vec{u}_{\parallel}$ (parallel to $\vec{k}_{\parallel}$). In order to determine how these appear in the scattering, we assume that the bulk Raman tensors control the scattering, as is also assumed in theories which make quantitative contact with previous data.[8] We then calculate the scattering due to the $u_{\perp}$ and $u_{\parallel}$ in the standard manner.[9] The results are also given in Table I. Note that our results indicate $u_{\parallel} > u_{\perp}$; the theory reviewed in Ref. 3 predicts this to be the case for values of ω intermediate between ω_{TO} and ω_S, the asymptotic SP frequency.

We note that the value of ϵ_∞ used in calculating the dispersion in Fig. 3 is somewhat higher than

TABLE I. Relative scattering intensities for surface polaritons in GaP for different combinations of incident and scattered light polarization and scattering direction. The numerical values are the experimental intensities, accurate to within approximately 40%, and the expressions enclosed by parentheses are the theoretical predictions. d is the constant element of the Raman tensor (see Ref. 9).

	$\vec{E}_0 \parallel \vec{E}_S$	$\vec{E}_0 \perp \vec{E}_S$
$\vec{k}_{\parallel} \parallel \hat{Y}$	1 ($\frac{2}{3}d^2\|u_{\perp}\|^2$)	2 ($\frac{2}{3}d^2\|u_{\parallel}\|^2$)
$\vec{k}_{\parallel} \parallel \hat{Z}$	3 ($\frac{1}{3}d^2\|u_{\perp}\|^2 + \frac{2}{3}d^2\|u_{\parallel}\|^2$)	< 0.2 (none)

other published values.[10] This causes the calculated dispersion curve to be higher than the experimental curve. We chose this value of ϵ_∞, however, because of the excellent fit it gives to the experimental points of Marschall and Fischer, which had very high experimental accuracy.[7] Since the sample thickness is ~10 times the penetration depth of SP in the present experiment, one expects no interaction between the SP of opposite faces. Thus there should be no separation into "upper" and "lower" modes, as in Ref. 1. The observed lowering of the frequency of the experimental points could, however, be explained by the effects of surface roughness.[11]

In conclusion, we have observed Raman scattering from surface polaritons at the surface of a single-crystal GaP sample. The Raman-scattering selection rules for SP were determined, and it was found that the Raman tensors for bulk modes are applicable to the SP, as long as the displacement components ($u_\perp$ and $u_\parallel$) of the SP are properly taken into account. Further work on the relative magnitudes of the SP displacement components, as a function of $k_\parallel$, and results for other surfaces of GaP will be presented in a longer paper, along with details of the experimental procedures used in the work reported in this Letter.[4]

We gratefully acknowledge many valuable discussions with Professor D. L. Mills and also thank H. W. Verleur of Bell Telephone Laboratories for the GaP crystal boule.

*Research supported by the U. S. Air Force Office of Scientific Research under Grant No. AFOSR 75-2760A.

[1]D. J. Evans, S. Ushioda, and J. D. McMullen, Phys. Rev. Lett. 31, 369 (1973); J.-Y. Prieur and S. Ushioda, Phys. Rev. Lett. 34, 1012 (1975).

[2]D. L. Mills and A. A. Maradudin, Phys. Rev. Lett. 31, 372 (1973).

[3]For a review of the theory of surface polaritons, see E. Burstein, A. Hartstein, J. Schoenwald, A. A. Maradudin, D. L. Mills, and R. F. Wallis, in *Polaritons*, edited by E. Burstein and F. de Martini (Pergamon, New York, 1974), p. 89.

[4]J. B. Valdez and S. Ushioda, to be published.

[5]S. Ushioda, J. B. Valdez, W. H. Ward, and A. R. Evans, Rev. Sci. Instrum. 45, 479 (1974).

[6]P. R. Bevington, *Data Reduction and Error Analysis for the Physical Sciences* (McGraw-Hill, New York, 1969), p. 204..

[7]See the remarks concerning the choice of ϵ_∞ and other parameters for GaP, in N. Marschall and B. Fischer, Phys. Rev. Lett. 28, 811 (1972).

[8]Y. J. Chen, E. Burstein, and D. L. Mills, Phys. Rev. Lett. 34, 1516 (1975); also D. L. Mills, Y. J. Chen, and E. Burstein, Phys. Rev. B 13, 4419 (1976).

[9]R. Loudon, Advan. Phys. 13, 423 (1964).

[10]M. Hass, for example, quotes a value $\epsilon_\infty = 8.46$, in *Semiconductors and Semimetals*, edited by R. K. Willardson and A. C. Beer (Academic, New York, 1967), Vol. 3, p. 14.

[11]The lowering of the frequencies of surface polaritons due to surface roughness has been predicted by A. A. Maradudin and W. Zierau, Phys. Rev. B 14, 484 (1976). An estimate based on their results indicates that the observed depression of ~0.5 cm^{-1} is quite reasonable for a mean surface roughness of 0.05 μm, the size of the final grit used to produce the samples in the present work. A depression of the surface-polariton dispersion curve has also been attributed to roughness by A. Hartstein and E. Burstein, Solid State Commun. 14, 1223 (1974).

ERRATA

FIRST-ORDER TORQUES AND SOLID-BODY SPINNING VELOCITIES IN INTENSE SOUND FIELDS. T. G. Wang, H. Kanber, and I. Rudnick [Phys. Rev. Lett. 38, 128 (1977)].

On Fig. 5 the ordinate should have a multiplication factor 0.032, and so should have the right-hand side of Eq. (2).